JMEPEG (2008) 17:127–133
DOI: 10.1007/s11665-007-9114-3

1059-9495/$19.00

Characterization of Hydrogen Permeation in Armco-Fe during Cathodic Polarization in Aqueous Electrolytic Media

Samuel M. Charca, Oswald N.C. Uwakweh, Basir Shafiq, and Vinod S. Agarwala

(Submitted January 3, 2007; in revised form February 21, 2007)

The study of hydrogen permeation behavior in Armco-Fe showed that 0.1 M H_2SO_4 was a more effective medium for cathodic polarization compared to 0.1 M NaOH. When both electrolytes were "poisoned" with 1.00 g/L $Na_2HAsO_4 \cdot 7H_2O$, as hydrogen recombination inhibitor, the corresponding hydrogen permeation levels were 3.5×10^{-5} A/cm^2 in 0.1 M H_2SO_4 while 0.75×10^{-5} A/cm^2 in 0.1 M NaOH. The breakthrough times were less than 30 s in 0.1 M H_2SO_4, while about 100 s in the NaOH. With varying amounts of "poisons", peak permeation of hydrogen (1.75×10^{-5} A/cm^2) was achieved with 10 g/L $Na_2HAsO_4 \cdot 7H_2O$ in 0.1 M H_2SO_4, while the least permeation resulted with 10 g/L (NH_2CSH_2) Thiourea addition for same level of 1.00 mA/cm^2 cathodic polarization.

Keywords Armco-Fe, cathodic polarization, hydrogen permeation, hydrogen recombination inhibitor agent (poison)

1. Introduction

Hydrogen interaction in iron and steel has been of interest to makers and users of these materials because these materials are known to suffer property losses and hence degradation in service performance when embrittled by hydrogen (Ref 1-3). In addition to hydrogen embrittlement that manifests in various ways, the formation of blisters in extreme cases can lead to catastrophic failures. In order to understand the problem of hydrogen interaction with iron and steel, different kinds of studies have been undertaken leading to considerable breakthroughs in the knowledge of hydrogen induced phenomena in iron and steels (Ref 4-6). For instance, the effect of hydrogen on mechanical properties conducted in an-situ manner where a materials property (e.g., tensile properties) was investigated while hydrogen was introduced into it as was carried out by Tiwari et al. (Ref 7). Similarly, the effect of hydrogen introduction in austenitic stainless steels where the austenitic phase decomposed to either a martensitic phase or other intermediate phases are well documented (Ref 8-14). In addition to these, the decomposition of superalloys, and, high-carbon binary Fe-C alloys due to the introduction of hydrogen well in line with the ones listed above have been verified as well by Uwakweh et al. (Ref 15-19).

In all these, nature of the electrolyte medium over which the cathodic polarization was effectuated primarily was of importance. Reported cases of hydrogen introduction characterized by the use of certain chemicals in controlled amounts in either an acid or a basic medium are well known (Ref 20-25). These chemicals are often referred to as hydrogen recombination inhibitor agents, charging promoters, or poisons. Their use in electrochemical hydrogen charging abound, as it has been proven that indeed, their presence facilitated tremendously, the process of hydrogen ingress (Ref 7, 14-19, 26-29). While the studies of the kinetics of the electrode reaction associated with the hydrogen charging have been of practical importance, most were solely focused on the use of known or proven amount of these promoters in the examination of the behavior of a known material with respect to the ingress of hydrogen. Since the permeation characteristic of hydrogen in iron and steel is of importance in the prediction of their performance in service, therefore the choice was made in this study to use Armco-Fe because, *it* can be viewed as a middle level material between pure iron and the multiphase martensitic/ferritic low-carbon steels. Further, given that hydrogen recombination inhibitors (or poisons) affect the ingress of hydrogen in metallic materials, this study was focused on the influence of known amounts of selected poisons on the hydrogen permeation behavior of Armco-Fe in the cold rolled/hot rolled and annealed states.

2. Experimental

The permeation experiments were carried out with the Devanathan and Stachurski (Ref 30-32) double cell (DSDC) with some modifications as shown in Fig. 1. To induce hydrogen charging from the entry or input-side, a DC power source with the current regulated to a pre-determined level by

Samuel M. Charca, Department of Civil Engineering, University of Puerto Rico – Mayagüez, P.O. Box 9044, Mayagüez 00681-9044, Puerto Rico; **Oswald N.C. Uwakweh,** and **Basir Shafiq,** Department of Engineering Science and Materials, College of Engineering, University of Puerto Rico – Mayagüez, P.O. Box 9044, Mayagüez 00681-9044, Puerto Rico; **Vinod S. Agarwala,** Naval Air Systems Command, 48110 Shaw Road, Bldg. 2187/Suite 237, Patuxent River, MD 20670-1906. Contact e-mail: uwakweh@ece.uprm.edu.

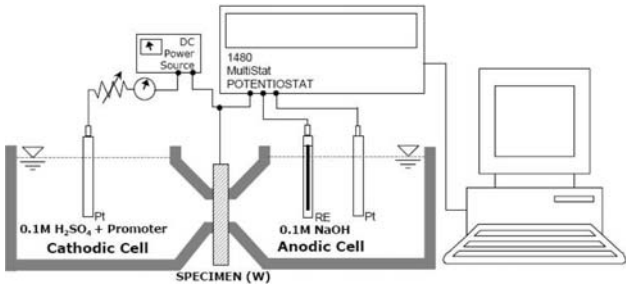

Fig. 1 Modified Devanathan and Stachurski double cell (DSDC)

Table 1 Weight composition of investigated material

Armco-Fe composition					
Materials	**C**	**Mn**	**S**	**P**	**Fe**
Comp. wt.%	0.012	0.60	0.05	0.05	Bal.

use of a variable resistance was employed. To record the hydrogen permeating through the membrane material (i.e., the sample), a Solartron 1480 Potentiostat which also ensured Galvanostatic or potentiostated conditions on the entry or exit sides of the membrane was employed. The membrane samples were Armco-Fe materials (with composition shown in Table 1) that were cut to 2.5 cm × 2.5 cm from a 10 cm × 10 cm As-received lots. The heat treatments that were carried out were done at 600 °C for 2 h followed by air cooling. The surfaces of the samples were successively polished with 320, 400, 600, and 800 grits, with a final 0.05 μalumina suspension with Chemomet cloths followed by rinsing in alcohol and blow air drying. To avoid deterioration of the surfaces, the samples were kept in a dessicator chamber. Prior to each charging, the samples were cleansed ultrasonically in methanol in order to remove possible contaminants on the surface which could otherwise affect the permeation process.

3. Results and Discussions

3.1 Typical Hydrogen Permeation Profile with DSDC

As said in the experimental, the DSDC arrangement derives its uniqueness in the sense that the membrane material (i.e., the Armco-Fe coupons) serves as the cathode of the input cell, while simultaneously serving as the anode of the exit cell. Under this arrangement, both sides were completed with inert platinum electrodes. The exit cell in this study was always operated with a 0.1 M NaOH electrolyte which is known to be mild on the steel material, i.e., does not provoke attack by corrosion during the course of a given experimental run. The exit side was first activated, by the use of the potentiostat which permitted extraction of residual hydrogen in the Armco-Fe. The extraction process was usually characterized by slight drop in anodic current leading to a stabilization stage with a current value of about 0.1 $\mu A/cm^2$ (Ref 6, 26, 29). Once this was achieved, then the input cell was filled with an appropriate electrolyte, followed by the adjusting of DC power source in order to obtain the desired cathodic polarization level. The

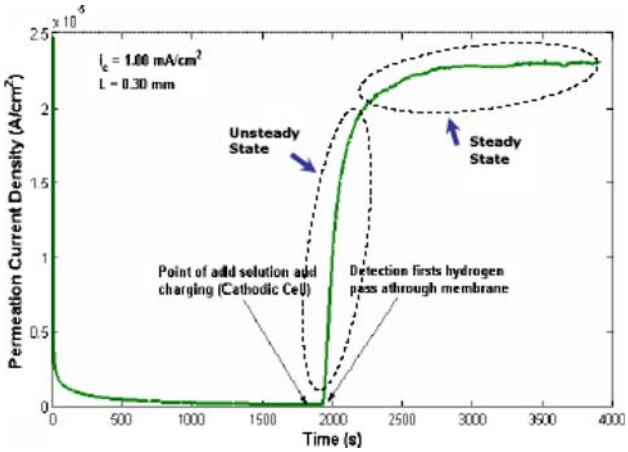

Fig. 2 Typical complete hydrogen permeation profile

system was thus left to run while the extraction current was recorded continuously. A typical permeation profile following this sequence is shown in Fig. 2. The abscissa reflected the amount of hydrogen extracted or permeating the material under study, while the ordinate axis recorded the time corresponding to the charging/permeation event.

The first portion of the plot shown in Fig. 2 represented the prior cathodic polarization extraction process (stabilization) which led to the elimination of hydrogen in solution in the material. After the indicated point of the introduction of the electrolyte on the input cell a time lapse existed before the permeation current was observed to increase. This increase in the permeation current will eventually reach a maximum value which will be subsequently referred to as the peak permeation value. The achieved peak permeation may or not remain steady due to a number of factors. If there was a decrease from the peak permeation, usually with time, a steady state value would have been achieved. The steady state permeation value could therefore be contrasted from the peak permeation value. This said, therefore, by examining the permeation profile of hydrogen through the membrane, important deduction about the material behavior could be made. This was because, as will be shown in subsequent results, the region marked as the "steady state" which corresponded to the transient or transient build up stage revealed also important materials related characteristics and hence, related to hydrogen transport behavior.

The breakthrough time, t_b, is the time taken from the introduction of the polarization current at the input-side to the first observed rise in the permeation from the extraction side. This corresponded to the time required for adsorbed hydrogen at the input-side to be dissolved in the material membrane, diffuse and emerge at the exit-side with the extraction process. From the knowledge of the breakthrough time, t_b, and time necessary to achieve peak permeation, one could determine the time necessary to achieve half of the peak permeation value or 99% of the value, which according to Devanathan and Stachurski (Ref 30-32), was denoted as $t_{1/2}$. By careful examination of the hydrogen permeation characteristics, it is possible to define an experimental standard that could become basis for reliable comparison of results from different sources, and also analyses of published data. These would be further highlighted in succeeding sections.

3.2 The Effect of Charging Medium (Same Amount of Promoter)

It was evident that the process that led to the liberation of hydrogen on the exposed surface of the material at the input-side was mere electrolysis, and as such its effectiveness was predicated upon ease of release of appropriate ionic species in the system. For instance, the permeation plots shown in Fig. 3 revealed that higher amounts of hydrogen permeated through similar membrane (0.20 mm thick, Armco-Fe that was heat treated at 600 °C for 2 h followed by air cooling) when the charging electrolyte was a 0.1 M H_2SO_4 with a 1.00 g/L $Na_2HAsO_4 \cdot 7H_2O$, than when same amount of 1.00 g/L $Na_2HAsO_4 \cdot 7H_2O$ was used to poison 0.1 M NaOH. The cathodic polarization current for both cases was 1.0 mA/cm^2, thereby showed that hydrogen dissolution and permeation was strongly affected by the type of polarizing medium despite the type of hydrogen recombination inhibitor employed during the charging process.

The dramatic difference between the accompanying hydrogen profiles were evident with respect to their breakthrough times, peak permeation levels, and nature of the transient build-up stages. Owing to the marked difference between the permeation profiles shown in Fig. 3, the need to determine an ideal hydrogen permeation profile was investigated. This resulted in the adoption of permeation profile shown in Fig. 2, to be the ideal one because upon attaining peak permeation, one did not observe a drop in permeation. Put differently, an ideal permeation profile should correspond to the case where the peak and steady state permeation levels would be equal. The permeation profile shown in Fig. 2 was established with a cathodic electrolyte that consisted of 0.1 M H_2SO_4 + 1.00 g/L $Na_2HAsO_4 \cdot 7H_2O$ with a polarizing current of 1.0 mA/cm^2. On the other hand, the behavior recorded with the 0.1 M NaOH + 1.00 g/L $Na_2HAsO_4 \cdot 7H_2O$ showed that hydrogen transport through the membrane was very sluggish, and correspondingly less amount of hydrogen diffused through the material. One possible reason for this could be limited hydrogen coverage of the exposed or charging surface due to the electrode kinetic reactions. It is evident from the profile that the dominating reaction in this case of 0.1 M H_2SO_4 based medium that hydrogen absorption and dissolution was much more enhanced. Further, the transient build up stage with the 0.1 MNaOH based medium having a "hump" indicated the occurrence of or presence of intermediate limited stage prior to the attainment of peak permeation level.

3.3 Effect of Varying Amount of $Na_2HAsO_4 \cdot 7H_2O$ in 0.1 M H_2SO_4

Furtherance to the preceding section, the effect of systematic increase in the amount of the $Na_2HAsO_4 \cdot 7H_2O$ poisoning agent in a 0.1 M H_2SO_4 on the hydrogen permeation on a 0.80 mm thick membrane was investigated. To help reveal how this chosen poison or promoter affected the hydrogen permeation behavior in the Armco-Fe. It can be noticed that the assembled permeation profile characteristics in the acid solution without promoter addition as summarized in Fig. 4 differed from the others.

It can be observed that the breakthrough times, t_b corresponding to the permeation profiles were not as widely different as were the cases shown in Fig. 3. This indicated that the initial coverage of the exposed surface under cathodic polarization was rather independent of the amount of promoter in the acid solution, while there were clearly distinct features associated with the early part of the transient build ups. Given that all the recorded permeation profiles were obtained with the same polarization current of 1.00 mA/cm^2, therefore, it can be deduced that there existed a threshold amount of promoter in a given medium required to achieve maximum hydrogen permeation. As shown in Fig. 4, the least hydrogen permeation was recorded with the charging medium that contained 10 g/L $Na_2HAsO_4 \cdot 7H_2O$ even in comparison to the poison free medium.

Further, it was observed that following the breakthrough time, the time lapse before accelerated build up decreased with increased amount of the promoter, even though it was not directly proportional to the quantity introduced. Without exception, the peak permeation states were followed by a decrease in permeation, which ultimately led to a steady state condition. Since the area under the permeation curve was proportional to the amount of hydrogen going through the material, therefore, it could be concluded that though the

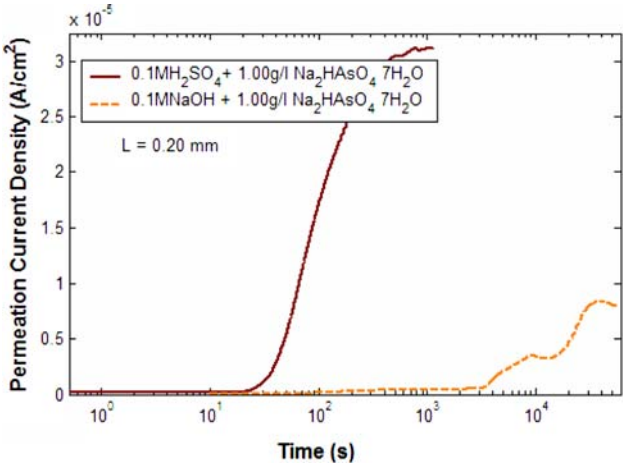

Fig. 3 Hydrogen permeation profile for two kinds of solution and same concentration of promoter

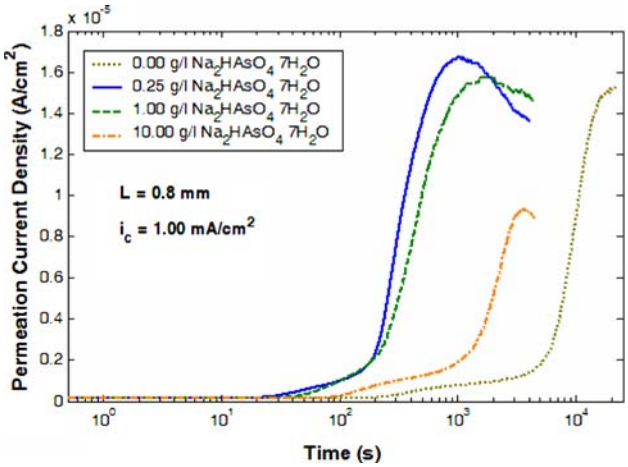

Fig. 4 Hydrogen permeation, obtained by the same concentration of 0.1 M H_2SO_4 with variation of promoter concentration

presence of the promoter facilitated hydrogen ingress, however, beyond a certain amount (10 g/L $Na_2HAsO_4 \cdot 7H_2O$) it would no longer impact the total amount of hydrogen in the material. From the consideration of time to achieve peak permeation, one noticed that promoter presence in an electrolyte accelerated hydrogen ingress into the material**.** The peak permeation values corresponding to the aforementioned measurements were summarized in Table 2.

3.4 Comparison of NaCN (Sodium Cyanide), Thiourea (NH_2CSNH_2) and Sodium Arsenate ($Na_2HAsO_4 \cdot H_2O$) in 0.1 M H_2SO_4 on the Permeation Behavior of Armco-Fe

Based on the observation that 0.1 M H_2SO_4 offered better or much more enhanced permeation of hydrogen than the 0.1 M NaOH medium, the effects of NaCN (Sodium Cyanide), Thiourea (NH_2CSNH_2) and Sodium Arsenate ($Na_2HAsO_4 \cdot 7H_2O$) hydrogen recombination inhibitors in 0.1 M H_2SO_4 were investigated. To facilitate the comparison of these promoters, they were investigated at two concentration levels, notably 1.0 and 10.0 g/L on the base 0.1 M H_2SO_4 electrolyte. The annealed material having a thickness of 0.78 mm was chosen for this study, while the cathodic polarization was maintained at 10 mA/cm^2 for each test. The recorded permeation profiles were displayed as shown in Fig. 5. The medium that conveyed the least peak hydrogen permeation was recorded with the solution containing 10.0 g/L NaCN, while the maximum peak hydrogen permeation was recorded with 1.0 g/L $Na_2HAsO_4 \cdot 7H_2O$ poisoned medium. The highest rate of rise in the transient build up was equally recorded for the 1.0 g/L $Na_2HAsO_4 \cdot 7H_2O$ poisoned medium. Apart from the 10.0 g/L NaCN medium that did not show a difference between peak and steady state permeation, all others displayed notable differences in the peak hydrogen permeation decay though to varying degrees. The medium that conferred comparable hydrogen permeation level to the ideal 1.0 g/L $Na_2HAsO_4 \cdot 7H_2O$ case was the10.0 g/L (NH_2CSNH_2) electrolyte, though characterized with smaller steep in the transient build up stage. Following the unsteady stage after breakthrough, the hydrogen permeation profile corresponding to the medium with 10.0 g/L $Na_2HAsO_4 \cdot 7H_2O$ poison displayed similar rate of transient stage build up irrespective of the protracted delay before the rise. On the strength of the marked differences observed for the investigated media, further investigation of the 1.0 g/L $Na_2HAsO_4 \cdot 7H_2O$ poisoned electrolyte was carried out because the corresponding hydrogen permeation profile for the polarization in this electrolyte medium yielded the best combination of breakthrough time and peak permeation level. The hydrogen transport associated with this medium did not show as much irregular behavior compared to the transport behaviors resulting from the polarization in the other media investigated.

Table 2 Summary of amount hydrogen permeated as a function of promoter concentration

Concentration, g/L, $Na_2HAsO_4 \cdot 7H_2O$	Total hydrogen (mol H/cm^2)
0.00[a]	2.01×10^{-6}
0.25[b]	5.64×10^{-7}
1.00[b]	5.78×10^{-7}
10.00[b]	2.14×10^{-7}

[a]Charging time t = 22,000.00 s
[b]Charging time t = 4000.00 s

3.5 Effect of Cathodic Polarization Current in 0.1 M H_2SO_4 Impregnated with 1.0 g/L $Na_2HAsO_4 \cdot 7H_2O$

The investigation of the hydrogen permeation behavior in a 1.0 g/L $Na_2HAsO_4 \cdot 7H_2O$ poisoned 0.1 M H_2SO_4 under varying cathodic polarizations were carried out on a 0.80 mm thick Armco-Fe with a prior 600 °C heat treatment followed by air cooling. The outcomes which were recorded in Fig. 6 showed a strong correlation between the hydrogen permeation profiles as a function of cathodic polarization. Close examination of the hydrogen permeation profiles showed that below 10.0 mA/cm^2 polarization current, hydrogen permeation displayed a delay before transient rise, while the delayed time decreased with increasing polarization current. Apart from the permeation profile with the 10.0 mA/cm^2 polarization current which showed decrease from the peak permeation, the other permeation profiles displayed equality in peak permeation and steady state values. In addition, the permeation profile obtained with the 10.0 mA/cm^2 polarization displayed "wavy" or irregular permeation upon attaining peak value over a period of more than 1000 s.

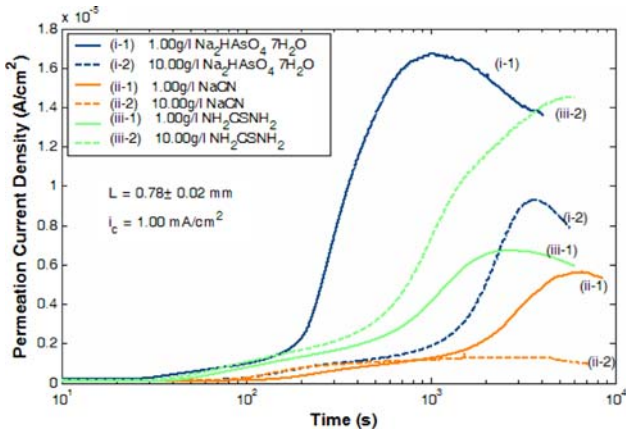

Fig. 5 Armco-Fe, hydrogen permeation profile subjected to different kinds of promoter

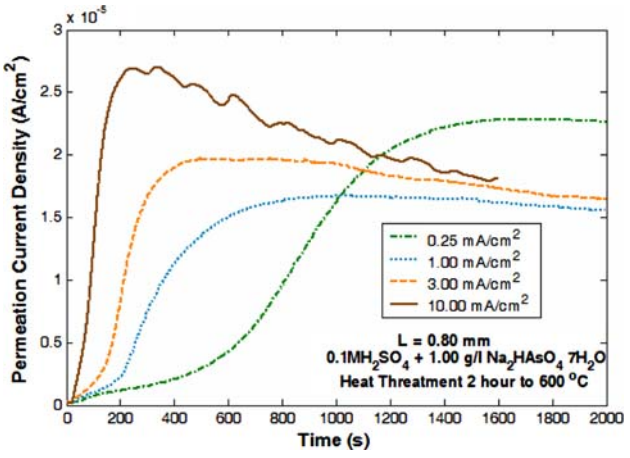

Fig. 6 Armco-Fe, hydrogen permeation subjected to different charging current

Comparison of the hydrogen permeation profiles showed differences at the peak permeation level and the shape of the unsteady state or transient build up stages as a function of cathodic polarization current density. Increasing cathodic polarization caused rapid rise in the permeation of hydrogen and also on the level of peak permeation observed. The permeation profiles for the 10.0 mA/cm^2 polarization showed a high-decay rate of 4.17×10^{-9} A/cm^2 s while attaining to a steady state level much lower than the steady state permeation level recorded with the 0.25 mA/cm^2 polarization current. On the other hand, the steady state permeation level for the 10.0 mA/cm^2 was observed to be slightly higher than those achieved with cathodic polarizations corresponding to the 1.00 and the 3.00 mA/cm^2 current densities, respectively.

Examination of the areas under the permeation curves, which is directly related to the amount of hydrogen in the material, revealed that the hydrogen content increased with increasing polarization current. However, the breakthrough times appeared to be independent of the cathodic polarization current in the same electrolyte medium. Further, one noticed that it was possible to identify two distinct portions of an entire permeation profile after the breakthrough to comprise an unsteady state and transient build up portions which depended on cathodic polarization currents. For the 10.00 mA/cm^2 polarization current profile, the transient build up stage seemed to be unique, while with the permeation curves obtained with the 3.00 and 1.00 mA/cm^2 charging currents, two portions indicated initial slow build up followed by a faster build up. On the other hand, the initial transient build up with the 0.25 mA/cm^2 was more extended in comparison to the permeation curves obtained with the 1.00 and 3.00 mA/cm^2 charging currents, respectively. The impact on the breakthrough time was summarized in Fig. 7, based on the deductions from Fig. 6.

3.6 Effect of Material Thickness on Hydrogen Permeation

Three characteristic material thicknesses measuring 0.40, 0.55, and 0.80 mm, respectively were charged under similar conditions involving the same cathodic polarization current of i_c = 1.00 mA/cm^2 in similar medium consisting of 0.1 M H_2SO_4 + 1.00 g/L $Na_2HAsO_4 \cdot 7H_2O$. As shown in Fig. 8, there was marked decrease in peak hydrogen permeation with increasing sample thickness. Furthermore it was observed that the tendency for permeation decay from peak level increased with decreasing sample thickness, while equality in peak permeation and steady state permeation occurred with thicker samples. This can be explained from the consideration of the dependence of hydrogen solubility with material thickness. It is generally easier to attain solubility limits with thinner metallic samples than thicker ones which by default contain more material defects and hence trapping sites. In line with this, the breakthrough times were determined to be 5, 11, and 30 s, respectively for the 0.40, 0.55, and 0.80 mm thick samples correspondingly.

4. Summarizing Discussion

The results presented thus far point to the fact that microstructure, polarization current, medium where the hydrogen charging was accomplished all affected the amount of hydrogen ingressed by the steel material in an electrochemical setting. The DSDC arrangement (Ref 6, 26, 29-31) was demonstrated to be a very effective, sensitive, and reliable means of introducing hydrogen in a metal and consequently in studying hydrogen transport behaviors in them. The presence of poisons (promoter) or hydrogen recombination inhibitors accelerated the process of hydrogen ingress, while there was a sensitivity vis-à-vis compatibility between material thickness and a given promoter. It was established that substantial amount of hydrogen could not be introduced in the Armco-Fe with NaCN in 0.1 M H_2SO_4, for instance, while this could well be the very opposite with another type of steel or metallic material.

A material sensitive variable could be deduced from the nature of transient build up portion, together with the nature of the decay that accompanied the peak permeation. The decay accompanying peak permeation was more pronounced with thicker materials and high-cathodic polarization currents. This implied that upon attainment of peak permeation, short circuits (i.e., other diffusion paths) or trapping sites acting as sinks (where atomic hydrogen recombined to form molecular hydrogen) become more influential since they become favorable regions for attracting hydrogen from the diffusing flux. These results collectively showed that care must be taken if the

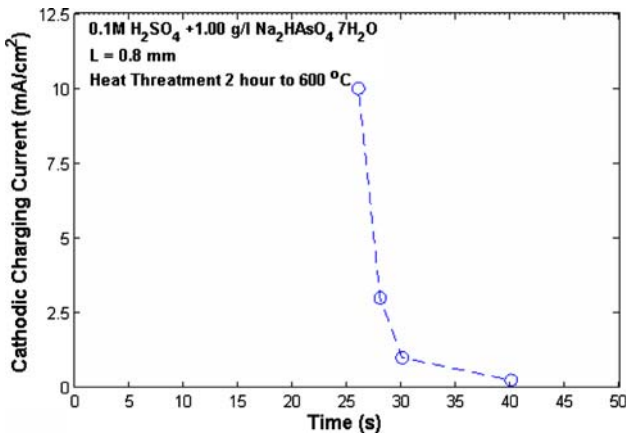

Fig. 7 Breakthrough time as a function of sample thickness, base in Fig. 6

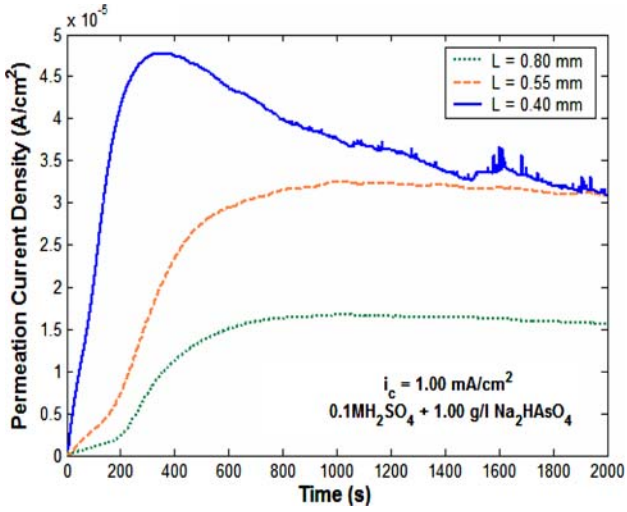

Fig. 8 Hydrogen permeation profile as a function for diverse sample thickness

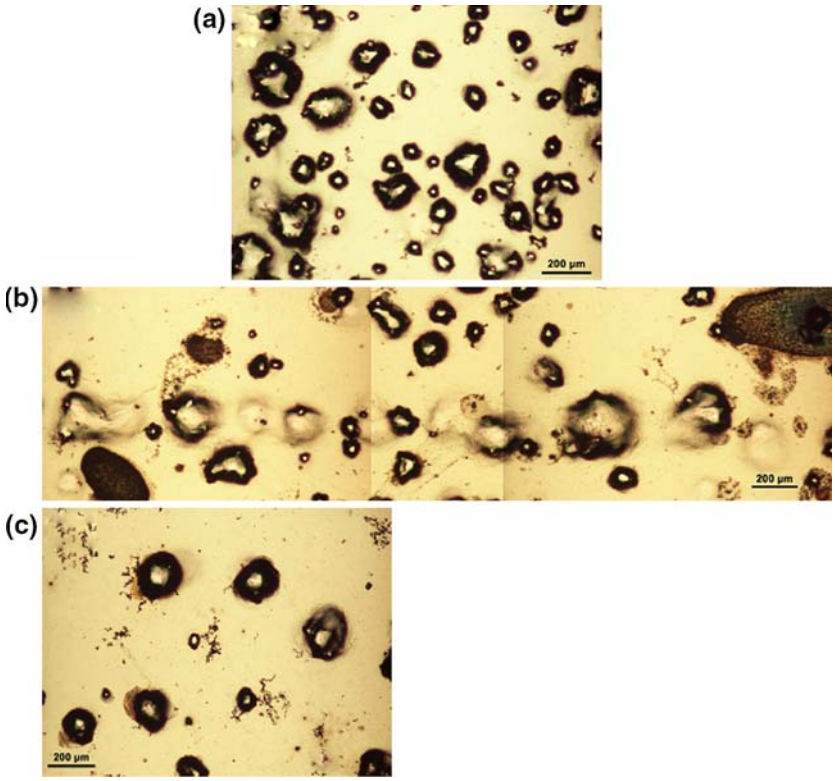

Fig. 9 Scanning electron images of cathodically charged Armco-Fe surfaces as a function of cathodic polarization current densities: (a) 10 mA/cm^2 (b) 3 mA/cm^2, and (c) 1 mA/cm^2, respectively

transport properties such as coefficient of diffusion and solubility limits of hydrogen in steels are to be determined based on the use of the DSDC in charging the steel membranes. This is because, these transport properties could only be determined with sufficient accuracies when extraneous factors such as influence of hydrogen recombination inhibitors, electrode kinetics (i.e., gas evolution) which affect the permeation behavior are well controlled (Ref 16-18, 26-33). Thus, there should be a prescribed standard requiring specifying polarization current, charging medium, and material thickness if this technique is used to determine transport properties of engineering materials. Equivalently, if this technique is used to determine diffusion properties or other transport properties, the actual experimental conditions detailing the charging medium, polarization current employed, material thickness, etc. must be detailed (Ref 34-38).

In the case of increasing the hydrogen cathodic polarization current, this caused increased hydrogen liberation, dwell time, and faster ingressing into the material. With this increase, there was correspondingly increased, formation of atomic hydrogen at the sub-surface which explained the formation of blisters—i.e., pocket of voids that were observed during the cathodic polarization of the Armco-Fe. There was a clear correlation between the amount of blister formed and the level of the cathodic polarization (i.e., charging current densities) employed in the hydrogen charging process (Ref 27, 28). The tendency for blister formation was observed to be higher when hydrogen cathodic charging was carried out with polarization current of 10.00 mA/cm^2 than with 3.00 and 1.00 mA/cm^2 levels respectively as shown in Fig. 9. The determination of the general conditions that tended to favor formation of blisters was in of itself a significant contribution of this study, given that blisters formation has serious consequences to the use of steels (Ref 39).

5. Conclusions

Based on the studies conduced on annealed Armco-Fe, the hydrogen transport as was characterized by permeation led to the following conclusions:

1. 0.1 M H_2SO_4 imbued with 1.00 g/L $Na_2HAsO_4 \cdot 7H_2O$ (sodium arsenate) was a more effective medium for enhanced hydrogen permeation than the lower level observed with poison concentration of 0.25 g/L and higher level of permeation observed with 10 g/L of $Na_2HAsO_4 \cdot 7H_2O$, respectively.
2. Peak hydrogen permeation could be accompanied by a decay or decrease in value due to the factors that affect hydrogen flux. The higher the rates of hydrogen build up, the higher the chances for hydrogen recombination at the material sub-surfaces, which led to the reduction in overall hydrogen peak permeation value. This was because of the synergistic relationship between hydrogen liberation, recombination, and diffusion flux tended to favor hydrogen atomic recombination at the subsurface of the material under charge.
3. The recombination of atomic hydrogen at the sub-surfaces led to the formation of blisters, or voids where molecular hydrogen accumulated, thereby prevented or hampered diffusion through the material.

4. Finally, the results of this study demonstrated that electrochemical means based on the modified DSDC arrangement was effective in the study of hydrogen transport behavior in steel material as evident in the case of Armco-Fe.

Acknowledgment

The authors, ONCU and BS would like to acknowledge support of ASEE through Summer Faculty program at different times, and also wishes to acknowledge the support of Dr. Yapa Rajapakse, the program manager of ONR-grant # N000140310540.

References

1. M. Bodenstein, Diffusion of Cathode Hydrogen through Iron and Platinum, *Z. Electrochem.*, 1922, **28**, p 517–526
2. A.R. Troiano, Embrittelement by Hydrogen and Other Interstitials, *Metal Progress*, 1960, **77**(2), p 112–117
3. R.P. Gangloff, *Comprehensive Structural Integrity*, vol. 6, I. Milne, R.O. Ritchie, and B. Ksrihalco, Eds. (New York, NY), Elsevier Science, 2003, p 31–101
4. D. Li, R.P. Gangloff, and J.R. Scully, Hydrogen Trap in Ultrahigh-Strength AERMET 100 Steel, *Metall. Mat. Trans. A*, 2004, **35A**, p 849–864
5. V.S. Agarwala, D.A. Berman, and G. Kohlhaas, "Cause and Prevention of Structural Materials Failure in Naval Environments," Paper 115, presented at CORROSION/84, (New Orleans, Louisiana, USA), 1984
6. V.S. Agarwala, An In-situ Experimental Study of the Mechanisms of Catastrophic Damage Phenomena, *Hydrogen Effects on Material Behavio*r, N.R. Moody and A.W. Thompson, Eds., The Minerals, Metals & Materials Society, 1990, p 1033
7. G.P. Tiwari, A. Bose, J.K. Chakravartty, S.L. Wadekar, M.K. Totlani, R.N. Arya, and R.K. Fotedar, Study of Internal Hydrogen Embrittlement of Steels, *Mater. Sci. Eng. A*, 2000, **286**, p 269–281
8. M.R. Louthan Jr. and R.G. Derrick, Hydrogen Transport in Austenitic Stainless Steels, *Corros. Sci.*, 1975, **15**(9), p 565–577
9. M.R. Louthan Jr., J.A. Donovan, and G.R. Caskey Jr., Tritium Absorption in Type 304L Stainless Steel, *Nucl. Technol.*, 1975, **26**(2), p 192–200
10. M.L. Holzworth and M.R. Louthan Jr., Hydrogen Induced Phase Transformations in Type 304L Stainless Steels, *Corrosion*, 1968, **24**(4), p 110–123
11. K. Kamachi, X-ray Study of Hydrides in Austenitic Stainless Steels, *J. Soc. Mater. Sci. Jpn.*, 1977, **26**(283), p 322–328, in Japanese
12. P. Kedzierzawski, Z. Szklarska-Smialowska, and M. Smialowski, Pulse Technique Employed for Studying Egress of Hydrogen from Iron Polarized Cathodically in As**3** Plus-containing Solutions, *J. Electrochem. Soc.*, 1980, **127**, p 2550–2555
13. K. Farrell and M.B. Lewis, The Hydrogen Content of Austenite After Cathodic Charging, *Scripta Metall.*, 1981, **15**, p 661–664
14. H. Hänninen, T. Hakkarainen, and P. Nenonen, *Hydrogen Effects in Metals,* J.M. Bernstein and A.W. Thompson, Eds., The Metallurgical Society of AIME, 1981, p 575–583
15. M. Hoelzel, S.A. Danilkin, H. Ehrenberrg, D.M. Toebbens, T.J. Udovic, H. Fues, and H. Wipf, Effects of High Pressure Hydrogen Charging on the Structure of Austenitic Stainless Steels, *Mater. Sci. Eng. A*, 2004, **384A**, p 255–261
16. A.J. Kumnick and H.H. Johnson, Steady State Hydrogen Transport Through Zone Refined Irons, *Metall. Trans A*, 1975, **6A**, p 1087–1091
17. N.R. Moody, S.L. Robinson, S.M. Myers, and F.A. Greulich, Deuterium Concentration Profiles in Fe-Ni-Co Alloys Electrochemically Charged at Room Temperature, *Acta Metall.*, 1989, **37**(1), p 281–290
18. S.L. Robinson, N.R. Moody, S.M. Myers, J.C. Farmer, and F.A. Greulich, The Effects of Current Density and Recombination Poisons on Electrochemical Charging of Deuterium into an Iron-Base Superally, *J. Electrochem. Soc.*, 1990, **137**(5), p 1391–1397
19. O.N.C. Uwakweh, "Distribution des interstitiels dans les Alliages Fe-C; Cinetique isochrone au cours du vieillissement des Martensites et Transformation induite par Chargement electronique d'Hydogene," Ph. D. Thesis, University of Nancy1 Nancy, France, 1990
20. O.N.C. Uwakweh, J.M.R. Genin, and J.F. Silvain, Hydrogen Charging of High Carbon Binary Steel and Martensitic Induced Transformation, *Scripta Metall.*, 1990, **24**(6), p 1075–1079
21. T.P Radhakrishnan and L.L. Shreir, Permeation of Hydrogen Through Steel by Electrochemical Transfer-1, *Electrochim. Acta*, 1966, **11**(8), p 1007–1021
22. J.F. Newman and L.L. Shreir, Role of Hydrides in Hydrogen Entry into Steel from Solution Containing Promoters, *Corros. Sci.*, 1969, **9**, p 631–641
23. R.D. McCright and R.W. Staehle, Effect of Arsenic Upon The Entry of Hydrogen Into Mild Steel as Determined at Constant Electrochemical Potential, *J. Electrochem. Soc.*, 1974, **121**(5), p 609–618
24. S.Y. Qian, B.E. Conway, and G. Jerkiewicz, Kinetic Rationalization of Catalyst Poison Effect on Cathodic H Sorption into Metals: Relation of Enhanced and Inhibition to Coverage, *J. Chem. Soc., Faraday Trans.*, 1998, **94**, p 2945–1954
25. M.H. Abd Elhamid, B.G. Ateya, K.G. Weil, and H.W. Pickering, Effect of Thiosulfate and Sulfite on the Permeation Rate of Hydrogen Through Iron, *Corrosion*, 2001, **57**(5), p 428–432
26. V.S. Agarwala and J.J. DeLuccia, Effect of Magnetic Field on Hydrogen Evolution and its Diffusion in Iron and Steel, *Proceeding of the 7th Int. Cong. On Metallic Corrosion* (Brasil) Hotel National/Rio de Janeiro, 1978, p 795–805
27. W.W. Gerberich, T. Livne, X.-F. Chen, and M. Kaczorowski, Crack Growth from Internal Hydrogen-Temperature and Microstructural Effects in 4340 Steel, *Metall. Trans. A*, 1988, **19A**, p 1310–1934
28. J. Barber and B.E. Conway, Structural Specificity of the Kinetics of the Hydrogen Evolution Reaction on the Low Index Surfaces of Pt Single-Crystal Electrodes in 0.5 m dm^{-3} NaOH, *J. Electroanal. Chem.*, 1990, **461**(1-2), p 80–89
29. S.M. Charca, "Study of Hydrogen Permeation and Diffusion in Steels: Predictive Model for Hydrogen Concentration," Master of Science Thesis, Department of Mechanical Engineering, University of Puerto Rico – Mayagüez, 2005
30. M.A.V. Devanathan and Z.O.J. Stachurski, The Adsorption and Diffusion of Electrolytic Hydrogen in Palladium, *Proc. Roy. Soc. Lond. Ser. A*, 1962, **A270**(1340), p 90–102
31. M.A.V. Devanathan, Z. Stachurski, and W. Beck, A Technique for the Evaluation of Hydrogen Embrittlement Characteristics of Electroplating Baths, *J. Electrochem. Soc.*, 1963, **110**(8), p 886–890
32. M.A.V. Devanathan and S. Venkatesen, Method for Measuring Hydrogen Permeation of Metals and its Application to Metal Finishing, *Int. Confer. Electrodepos. Metal Finish.*, 1964, **42**, p 123–128
33. J.J. DeLuccia, *Electrochemical Aspects of Hydrogen in Metals: Hydrogen Embrittlement: Prevention and Control*, ASTM STP 962, L. Raymond, Ed. (Philadelphia), American Society for Testing and Materials, 1988, p 17–34
34. ASTM G 148: Standard Practice for Evaluation of Hydrogen Uptake, Permeation, and Transport in Metals by an Electrochemical Technique
35. J.O'M. Bockris, J. McBreen, and L. Nanis, The Hydrogen Evolution Kinetics and Hydrogen Entry into α-iron, *J. Electrochem. Soc.*, 1965, **112**(101), p 1025–1031
36. T. Zakroczymski, Electrochemical Determination of Hydrogen in Metals, *J. Electroanal. Chem.*, 1999, **475**, p 82–88
37. J. Flis, T. Zakroczymski, V. Kleshnya, T. Kobiela, and R. Dus, Changes in Hydrogen Entry and in Surface of Iron during Cathodic Polarisation in Alkaline, *Electrochim. Acta*, 1999, **44**(23), p 3989–3997
38. E. Owczarek and T. Zakroczymski, Hydrogen Transport in Duplex Stainless Steel, *Acta*, 2000, **48**(12), p 3059–3070
39. Nace technical report: Item No. 24185, NACE International Publication 8X294 (2003 Edition)